applied optics

Dual-wavelength passively Q-switched Nd:GYSGG laser by tungsten disulfide saturable absorber

Y. J. Gao,[1] B. Y. Zhang,[1,*] Q. Song,[1] G. J. Wang,[1] W. J. Wang,[1] M. H. Hong,[1] R. Q. Dou,[2] D. L. Sun,[2] and Q. L. Zhang[2]

[1]School of Physics Science and Information Engineering, Shandong Key Laboratory of Optical Communication Science and Technology, Liaocheng University, Liaocheng 252059, China
[2]The Key Laboratory of Photonic Devices and Materials of Anhui, Anhui Institute of Optics and Fine Mechanics, Chinese Academy of Sciences, Hefei 230031, China
*Corresponding author: bingyuanzhang@yahoo.com

Received 18 March 2016; revised 17 May 2016; accepted 25 May 2016; posted 27 May 2016 (Doc. ID 261451); published 17 June 2016

A dual-wavelength passively Q-switched Nd:GYSGG laser using vacuum evaporating tungsten disulfide (WS_2) as a saturable absorber was demonstrated for the first time to the best of our knowledge. The WS_2 saturable absorber was prepared simply by evaporating nanometer WS_2 powders onto a quartz substrate in a vacuum. By inserting the WS_2 saturable absorber into the laser cavity, stable Q-switched laser operation was achieved with a maximum average output power of 367 mW, a pulse repetition rate of 70.7 kHz, the shortest pulse width of 591 ns, and pulse energy of about 1.05 μJ. By vacuum evaporation method, a high-quality WS_2 saturable absorber can be produced, and it seems to be a suitable method for fabrication of 2D transition metal dichalcogenides.

OCIS codes: (140.3480) Lasers, diode-pumped; (140.3580) Lasers, solid-state; (140.3380) Laser materials.

http://dx.doi.org/10.1364/AO.55.004929

1. INTRODUCTION

Passive Q-switching is an effective technology for the generation of nanosecond pulses, and the saturable absorber (SA) is an essential device in a passively Q-switched laser. Different SA materials such as semiconductor saturable absorption mirrors [1,2], graphene [3–5], and graphene oxide [6–8] have been studied for some years. Two-dimensional transition metal dichalcogenides (TMDCs) have attracted interest due to their extraordinary properties and various applications. They are applied as lubricants [9], catalysts [10], and electrode materials [11,12] owing to their good electronic, optical, mechanical chemical, and thermal properties [13–17]. TMDCs are a series of materials with the formula MX_2. They can form layered structures of the form X-M-X and exist in bulk form as stacks of strongly bonded layers with a weak interlayer [18]. WS_2, WSe_2, WTe_2, and MoS_2 are typical TMDCs. Graphene-like WS_2 is regarded as a saturable absorber for passively Q-switching to generate nanosecond pulses in a broadband absorption spectral range owing to an ultrafast saturable absorption and ultrahigh optical damage threshold [19]. Researchers have developed many methods to fabricate few-layer WS_2 nanosheets, such as pulsed-laser deposition [20], chemical vapor [21], hydrothermal intercalation exfoliation [22], and mechanical exfoliation [23,24]. Compared with mechanical exfoliation [25], the virtues of vacuum evaporation method are uniformity and stability. Dual-wavelength Q-switched lasers have wide applications in different fields [26,27]. The disordered structure, the lower emission cross sections and longer upper-laser-level lifetime of Nd:GYSGG crystal are beneficial to generate nanosecond and dual-wavelength laser pulse. Recently, black phosphorous (BP) has attract more attention owing to its strong light–matter interaction, narrow direct bandgap, and wide range of tunable optical response. Multilayer BPs could be developed as another new type of 2D saturable absorber with operation bandwidth ranging from the visible (400 nm) toward mid-IR (at least 1930 nm) being reported [28].

In this paper, a vacuum evaporation method was employed to fabricate a WS_2 saturable absorber for the first time to our knowledge. A stable Q-switched Nd:GYSGG laser operation was achieved with a maximum average output power of 367 mW, pulse repetition rate of 362 kHz, shortest pulse width of 591 ns, and single pulse energy of about 1.05 μJ. The output spectrum peaked at 1057 and 1061 nm also has been measured.

2. PREPARATION AND CHARACTERIZATION OF WS_2 SATURABLE ABSORBER

A WS_2 saturable absorber was prepared by the vacuum evaporation method. 0.05 g WS_2 powders were uniformly laid on an

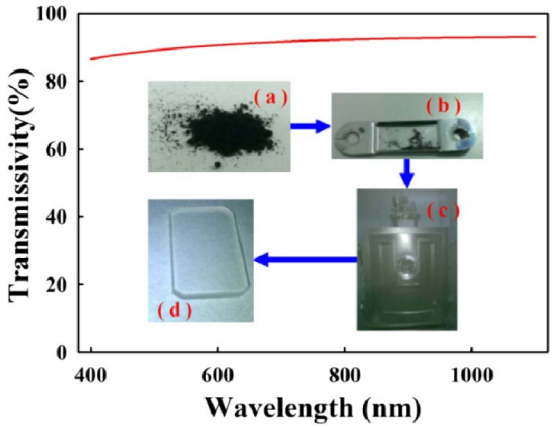

Fig. 1. UV-Vis-NIR transmissivity spectrum of WS_2 saturable absorber (insert preparation process).

evaporator boat. Then, the evaporator boat was put in an electron team evaporation and voltage evaporation hybrid coating system (DZS-500), air of the device was vacuumized until the vacuum chamber in a stable state with pressure of 1.0 E^{-3} Pa. After that, an evaporator source current began to increase at a speed of 0.5 A per second and suspend 2 min per 50 A. We can obtain a WS_2 saturable absorber with the thickness of 120 nm by evaporating 5 h with 190 A current.

Figure 1 shows the preparation process and UV-Vis-NIR transmissivity spectrum of the WS_2 saturable absorber; the transmissivity of the saturable absorber was characterized by the UV-Vis-NIR spectrophotometer. As depicted in Fig. 1, a WS_2 nanosheet was regarded as a saturable absorber in a wide wavelength range from 400 to 1100 nm. The transmissivity of this SA was 92.7% and 93% at 1057 nm and 1061 nm, respectively.

Surface morphology of WS_2 SA was measured by atomic force microscopy (AFM) and Raman spectra. The Raman spectrometer (RM 2000) was used to measure the Raman spectrum of the WS_2 saturable absorber. Figure 2 shows the Raman spectrum of the deposited WS_2 SA. Two Raman peaks can be identified in this spectrum: the characteristic bands at 345 cm^{-1} and 415 cm^{-1} are assigned to the in-plane (E_2g) and out-of-plane (A_1g) vibrational modes of WS_2 [29]. A typical

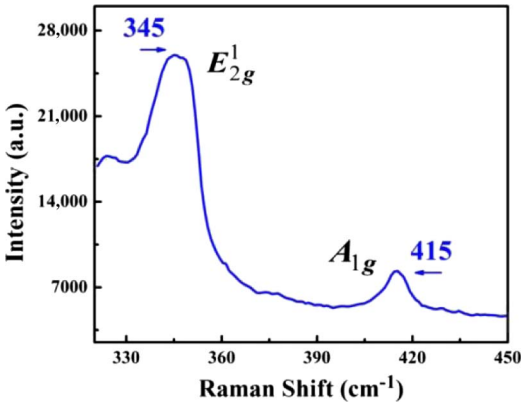

Fig. 2. Raman spectrum of the WS_2 saturable absorber.

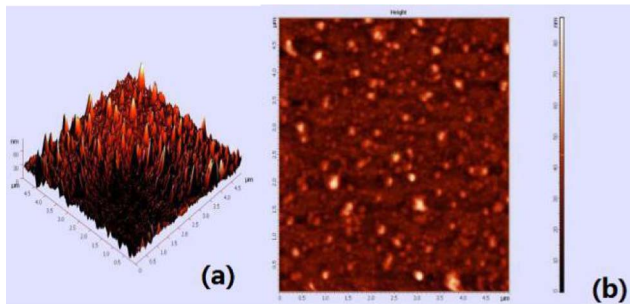

Fig. 3. AFM image of WS_2 SA: (a) 3D, (b) 2D.

3D AFM image of WS_2 SA is shown in Fig. 3(a), and the corresponding 2D AFM image is shown in Fig. 3(b).

3. SETUP OF THE DIODE-END-PUMPED ND:GYSGG LASER

Figure 4 shows a schematic of the experimental setup. The passively *Q*-switched laser setup was based on a linear cavity with the length of 18 mm. The pump source of the experiment was a fiber-coupled laser diode (LD) with a central wavelength of 808 nm. The pump beam was focused into the Nd:GYSGG crystal with a spot radius of about 0.1 mm using a focusing system. The mirror M was the input coupler (HT at 808 nm and HR at 1.06 μm). The Nd:GYSGG crystal with the dimensions of 3 mm × 3 mm × 5 mm was used in the experiment. The WS_2 nanosheet was employed as the saturable absorber. The mirrors OC (output coupler) with different transmissions of 15% and 27% at 1.06 μm were employed, respectively. The laser pulses were detected by a fast photodetector (ET-3000) and an oscilloscope (Agilent DSO54832b).

4. EXPERIMENTAL RESULTS AND DISCUSSIONS

During the experiment, the WS_2 saturable absorber was inserted into the laser cavity to generate ultrashort pulses. When the pump power increases to 3 W, *Q*-switched operation can be obtained. In order to protect the crystal, the maximum pump power is 4 W.

The relationship of the output power and pump power of the continuous wave (CW) and *Q*-switched (QS) operation is shown in Fig. 5. We can see that the optical-to-optical conversion efficiencies decrease from 9.2% to 7.5% for QS and 20% to 18% for CW with the transmissions of the output

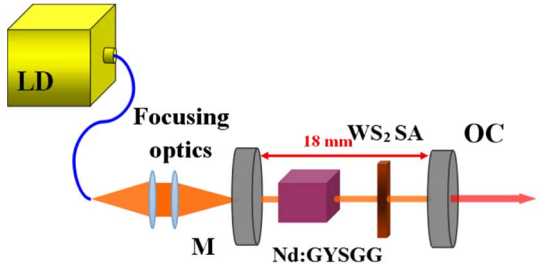

Fig. 4. Schematic setup of the Nd:GYSGG laser.

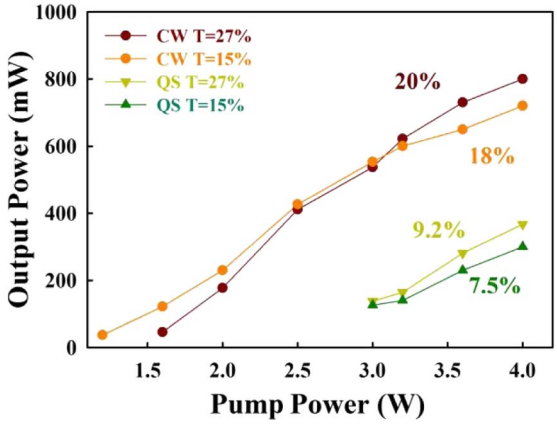

Fig. 5. Variation of the output power and pump power under different conditions.

couplers decreasing from 27% to 15%. The O-to-O efficiency for the CW laser was 20% and 18% with different output couplers and for the highest output power. The slope efficiencies for CW and QS laser are 31.4%, 24.9% and 36.7%, 30%. Under the pump power of 4 W, the maximum output powers of 367 and 300 mW were obtained for *Q*-switched operation with two different output couplers (27%, 15%).

From Fig. 6, we see that the pulse width decreased with the increasing of pump power. The minimum pulse widths of 620 and 591 ns were obtained with the output transmissions of 15% and 27%, respectively, under the pump power of 4 W. Under the same conditions, the repetition rate of 67.35 and 70.7 kHz were attained. The pulse width decreased from 1050 to 620 ns and 1000 to 591 ns, respectively, with the pump power increasing from 3 to 4 W with the output transmissions of 15% and 27%, respectively. Moreover, the repetition rate increased with the increasing of pump power and the transmissions of the output couplers, respectively. The repetition rate changed from 35 to 67.35 kHz and from 45 to 70.7 kHz with the pump power increasing from 3 to 4 W with the output transmissions of 15% and 27%, respectively. The higher repetition rate due to the short absorption recovery time and low saturable energy intensity of WS_2 SA. Under the same

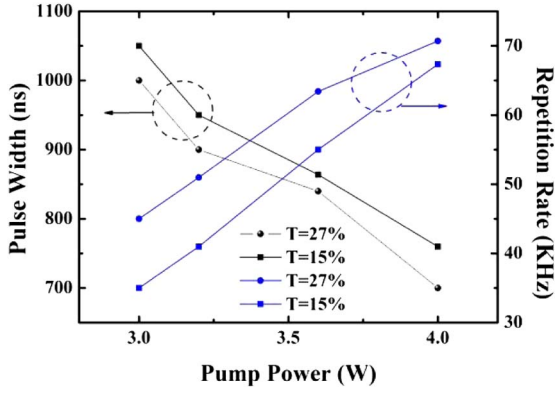

Fig. 6. Variation of the pulse width and repetition rate with the pump power.

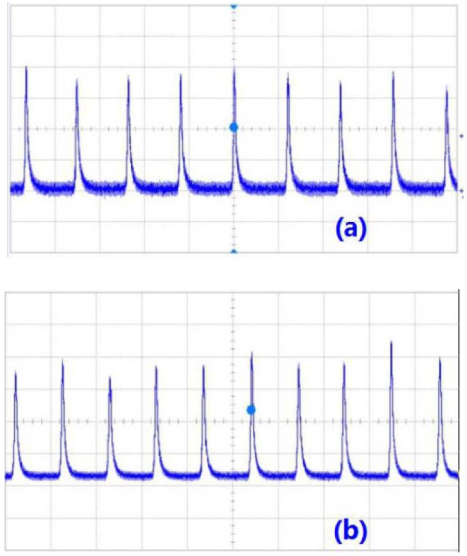

Fig. 7. Pulse train of *Q*-switched Nd:GYSGG laser with the (a) 15% output coupler (b) 27% output coupler (20 μs/div).

pump power of 4 W, the single pulse energy is 4.45 and 5.19 μJ with the output transmissions of 15% and 27%, respectively, the corresponding peak power are 5.86 and 7.42 W, respectively.

Figures 7 and 8 show the typical pulse train and typical single pulse of *Q*-switched operation with the 15% and 27% output couplers. The pulse train is stable with few amplitude jitters. The typical single pulses width are 620 and 591 ns, respectively.

The output spectrum with the output transmissions of 15% and 27% are shown in Fig. 9, which were measured by an Ocean Optics HR2000+ spectrum analyzer. Two laser lines are found simultaneously at 1057 and 1061 nm. The separation between wavelengths is quite stable.

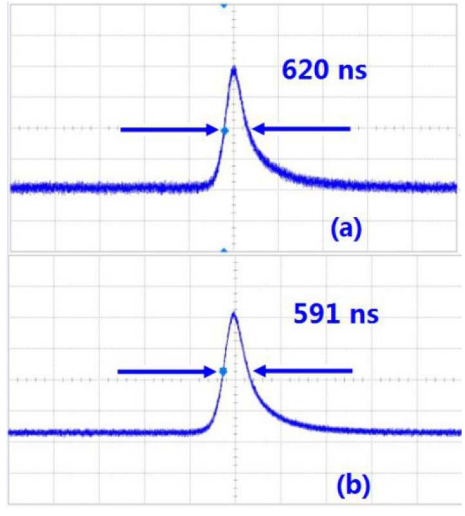

Fig. 8. Typical single pulse of *Q*-switched Nd:GYSGG laser with (a) 15% output coupler (b) 27% output coupler (1 μs/div).

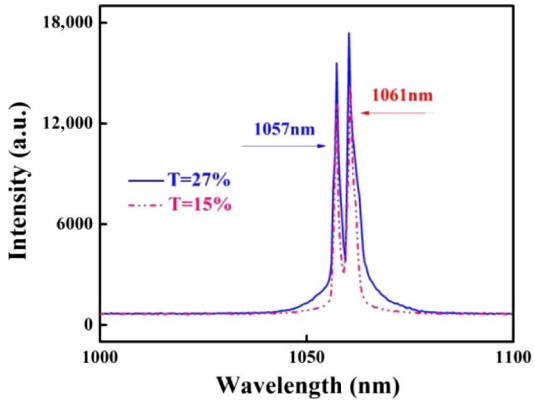

Fig. 9. Output spectrum of passively *Q*-switched Nd:GYSGG laser.

5. CONCLUSION

In this paper, we have reported a stable passively *Q*-switched dual-wavelength Nd:GYSGG laser with a WS_2 saturable absorber. The output spectrum peaked at 1057 and 1061 nm has been measured. The maximum average output power was 367 mW, and the shortest pulse width of 591 ns was achieved by using the output coupler of 27% under the pump power of 4 W. Meanwhile, a vacuum evaporation method to fabricate a WS_2 saturable absorber was achieved. In addition, the vacuum evaporation method seems to be a suitable method for fabrication of 2D transition metal dichalcogenides.

Funding. National Natural Science Foundation of China (NSFC) (61275147, 11375081, 51172236); Natural Science Foundation of Shandong Province (ZR2014FL030); Special Construction Project Fund for Shandong Province Taishan Mountain Scholar.

REFERENCES

1. D. J. Maas, B. Rudin, A.-R. Bellancourt, D. Iwaniuk, and S. V. Marchese, "High precision optical characterization of semiconductor saturable absorber mirrors," Opt. Express **16**, 7571–7579 (2008).
2. U. Keller, K. J. Weingarten, and F. X. Kärtner, "Semiconductor saturable absorber mirrors (SESAM's) for femtosecond to nanosecond pulse generation in solid-state lasers," IEEE J. Sel. Top. Quantum **2**, 435–453 (1996).
3. S. Husaini and R. G. Bedford, "Graphene saturable absorber for high power semiconductor disk laser mode-locking," Appl. Phys. Lett. **104**, 161107 (2014).
4. S. C. Xu, B. Y. Man, and S. Z. Jiang, "Sapphire-based graphene saturable absorber for long-time working femtosecond lasers," Opt. Lett. **39**, 2707–2710 (2014).
5. H. Ahmad, F. D. Muhammad, and M. Z. Zulkifli, "Wideband tunable *Q*-switched fiber laser using graphene as a saturable absorber," J. Mod. Opt. **60**, 1563–1568 (2013).
6. L. Kornaszewski, G. Maker, G. P. A. Malcolm, M. Butkus, E. U. Rafailov, and C. J. Hamilton, "Composite chromium and graphene oxide as saturable absorber in ytterbium-doped *Q*-switched fiber lasers," Appl. Opt. **53**, 1173–1180 (2014).
7. R. Mary, G. Brown, S. J. Beecher, R. R. Thomson, D. Popa, Z. Sun, F. Torrisi, T. Hasan, S. Milana, F. Bonaccorso, A. C. Ferrari, and A. K. Kar, "High-energy passively *Q*-switched 2 μm Tm^{3+}-doped double-clad fiber laser using graphene-oxide-deposited fiber taper," Opt. Express **21**, 204–209 (2013).
8. H. Ahmad, A. Z. Zulkifli, and Y. Y. Kiat, "*Q*-switched fibre laser using 21 cm Bismuth-erbium doped fibre and graphene oxide as saturable absorber," Opt. Commun. **310**, 53–57 (2014).
9. L. Rapport, Y. Bilik, and M. Homyonfer, "Hollow nanoparticles of WS_2as potential solid-state lubricants," Nature **387**, 791–793 (1997).
10. M. Mdleleni, H. A. Taeghwan, and K. S. Suslick, "Sonochemical synthesis of nanostructured molybdenum sulfide," J. Am. Chem. Soc. **120**, 6189–6190 (1998).
11. M. Chhowalla, H. S. Shin, G. Eda, L. J. Li, K. P. Loh, and H. Zhang, "The chemistry of two-dimensional layered transition metal dichalcogenide nanosheets," Nat. Chem. **5**, 263–275 (2013).
12. W. S. Leong, X. Luo, Y. Li, K. H. Khoo, S. Y. Quek, and J. T. L. Thong, "Low resistance metal contacts to MoS_2 devices with nickel-etched-graphene electrodes," ACS Nano **9**, 869–877 (2015).
13. H. Zhang, Z. Sun, and J. Wang, "Introduction to the photonics based on two-dimensional materials feature issue," Photon. Res. **3**, PBTD1 (2015).
14. F. Gianluca, B. Francesco, L. Giuseppe, P. Tomás, N. Daniel, and S. Alan, "Electronics based on two-dimensional materials," Nat. Nanotechnol. **9**, 768–779 (2014).
15. A. Rosenberg, R. J. Tonucci, H. B. Lin, and A. J. Campillo, "Near-infrared two-dimensional photonic band-gap materials," Opt. Lett. **21**, 830–832 (1996).
16. H. Zhang, S. B. Lu, and J. Zheng, "Molybdenum disulfide (MoS_2) as a broadband saturable absorber for ultra-fast photonics," Opt. Express **22**, 7249–7260 (2014).
17. D. Mao, S. L. Zhang, Y. D. Wang, X. T. Gan, W. D. Zhang, and T. Mei, "WS_2 saturable absorber for dissipative soliton mode locking at 1.06 and 1.55 μm," Opt. Express **23**, 27509–27519 (2015).
18. Q. H. Wang, K. Kalantar-Zadeh, A. Kis, J. N. Coleman, and M. S. Strano, "Electronics and optoelectronics of two-dimensional transition metal dichalcogenides," Nat. Nanotechnol. **7**, 699–712 (2012).
19. V. Vega-Mayoral, C. Backes, D. Hanlon, U. Khan, Z. Gholamvand, M. O'Brien, G. S. Duesberg, C. Gadermaier, and J. N. Coleman, "Photoluminescence from liquid-exfoliated WS_2 monomers in poly(vinyl alcohol) polymer composites," Adv. Funct. Mater. **26**, 1028–1039 (2015).
20. J. D. Yao, Z. Q. Zheng, J. M. Shao, and G. W. Yang, "Stable, highly-responsive and broadband photodetection based on large-area multilayered WS_2 films grown by pulsed-laser deposition," Nanoscale **7**, 14974–14981 (2015).
21. C. Cong, J. Shang, X. Wu, B. Cao, N. Peimyoo, and C. Qiu, "Synthesis and optical properties of large-scale single-crystalline two-dimensional semiconductor WS_2 monolayer from chemical vapor deposition," Adv. Opt. Mater. **2**, 131–136 (2013).
22. S. Wang, G. Li, Y. He, H. Yin, Z. Xu, and B. Zou, "Cobalt-doped disulfide nanotubes prepared by exfoliation-intercalation–hydrothermal adulteration," Mater. Lett. **60**, 815–819 (2008).
23. Y. Kobayashi, S. Sasaki, S. Mori, H. Hibino, Z. Liu, K. Watanabe, and T. Taniguchi, "Growth and optical properties of high-quality monolayer WS_2 on graphite," ACS Nano **9**, 4056–4063 (2008).
24. D. Mao, Y. D. Wang, C. J. Ma, L. Han, B. Q. Jiang, and X. T. Gan, "WS_2 mode-locked ultrafast fiber laser," Sci. Rep. **5**, 7965 (2014).
25. R. Wang, H. C. Chien, J. Kumar, N. Kumar, H. Y. Chiu, and H. Zhao, "Third-harmonic generation in ultrathin films of MoS_2," ACS Appl. Mater. Interface **6**, 314–318 (2013).
26. Y. G. Zhao, X. Li, and M. Xu, "Dual-wavelength synchronously q-switched solid-state laser with multi-layered graphene as saturable absorber," Opt. Express **21**, 3516–3522 (2013).
27. A. Klehr, H. Wenzel, O. Brox, S. Schwertfeger, R. Staske, and G. Erbert, "Dynamics of a gain-switched distributed feedback ridge waveguide laser in nanoseconds time scale under very high current injection conditions," Opt. Express **21**, 2777–2786 (2013).
28. S. B. Lu, L. L. Miao, Z. N. Guo, X. Qi, C. J. Zhao, H. Zhang, and D. Y. Fan, "Broadband nonlinear optical response in multi-layer black phosphorus: an emerging infrared and mid-infrared optical material," Opt. Express **23**, 11183–11194 (2015).
29. P. Néstor, E. A. Laura, B. Ayse, C. Andres, H. R. Gutiérrez, and S. Feng, "Photosensor device based on few-layered WS_2 films," Adv. Funct. Mater. **23**, 5511–5517 (2013).